

Supporting Information

The structure of dynamic, taxol-stabilized, and GMPPCP-stabilized microtubules

Avi Ginsburg,^{†,‡,¶,⊥} Asaf Shemesh,^{†,¶,⊥} Abigail Millgram,^{†,¶} Raviv Dharan,^{†,§} Yael Levi-Kalisman,^{||,¶} Israel Ringel,^{‡,§} and Uri Raviv^{*,†,¶}

Institute of Chemistry, The Hebrew University of Jerusalem, Jerusalem, 9190401, Israel, Institute for Drug Research, School of Pharmacy, The Hebrew University of Jerusalem, 9112102, Jerusalem, Israel, Center for Nanoscience and Nanotechnology, The Hebrew University of Jerusalem, Jerusalem, 9190401, Israel, Azrieli College of Engineering, Jerusalem, 9103501, Israel, and Institute of Life Sciences, The Hebrew University of Jerusalem, Jerusalem, 9190401, Israel

E-mail: uri.raviv@mail.huji.ac.il

Phone: +972 (2) 6586030. Fax: +972 (2) 5660425

Additional cryo-TEM images

Figures S1 - S6 show additional examples to the cryo-TEM images shown in Figures 1 - 3.

*To whom correspondence should be addressed

[†]HUJI1

[‡]HUJI2

[¶]HUJI4

[§]Azrieli

^{||}HUJI3

[⊥]These authors contributed equally to this work

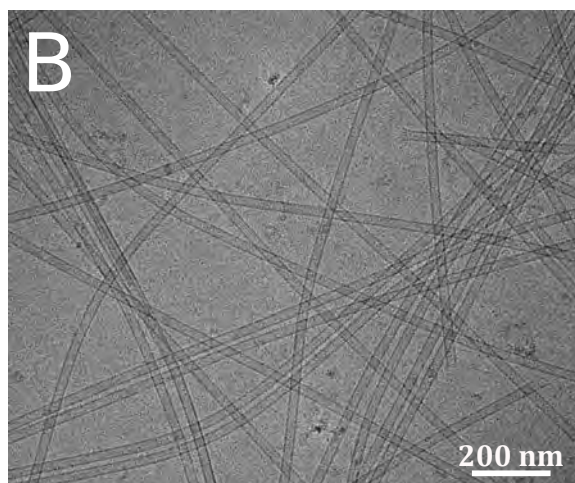
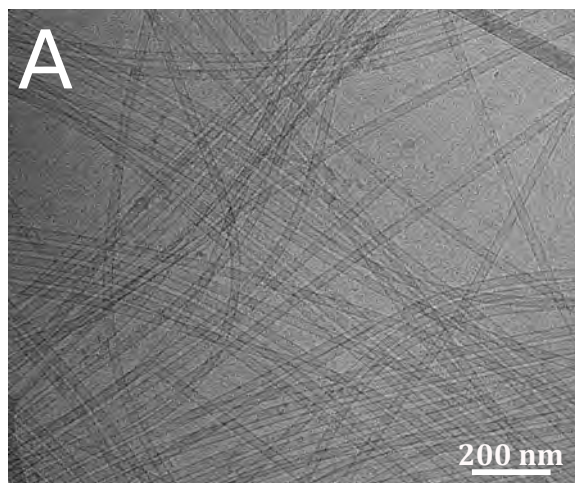


Figure S1: Cryo-TEM images (A & B) of dynamic MT solution. A solution of 0.2mM tubulin was polymerized for 35 min at 36 °C in the presence of 4mM GTP. An aliquot was extracted, kept at 36 °C for 90min, until being vitrified and imaged.

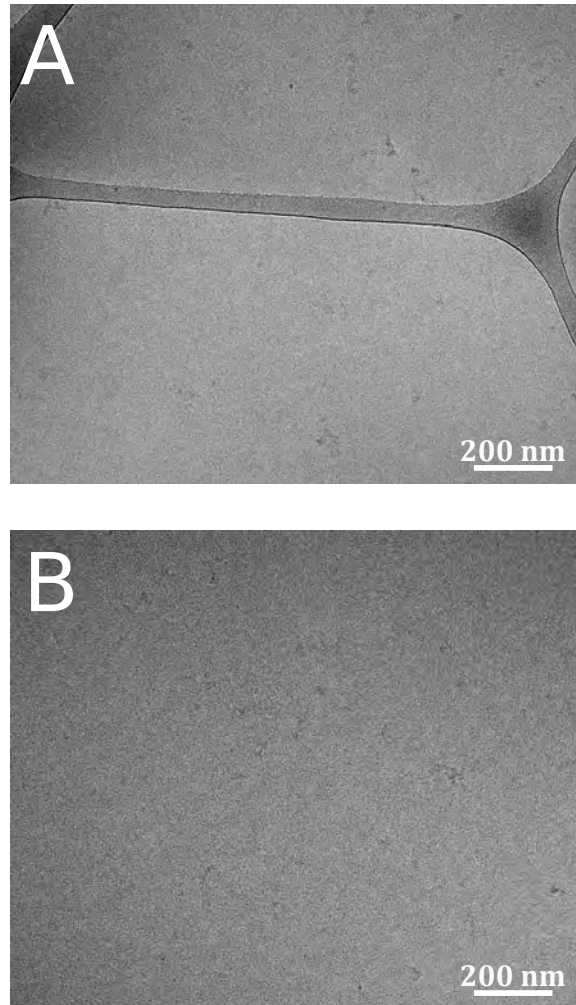


Figure S2: Cryo-TEM images (A & B) of dynamic MT supernatant. A solution of 0.2 mM tubulin was polymerized for 35 min at 36°C in the presence of 4 mM GTP. The MT solution was then centrifuged at 20800g, at 36°C for 30 min. Supernatant sample was extracted, and kept at 36°C for 60 min, until being vitrified and imaged.

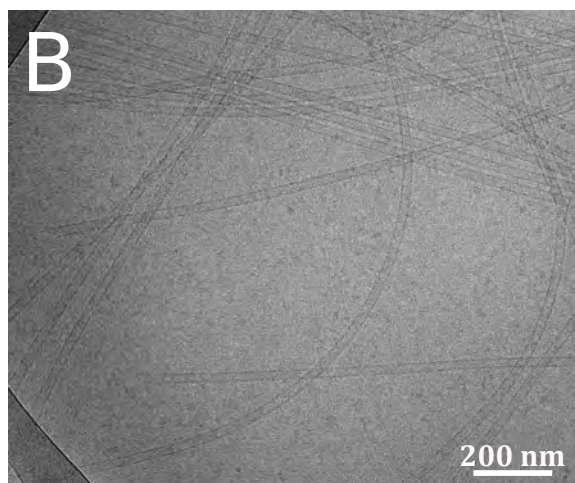
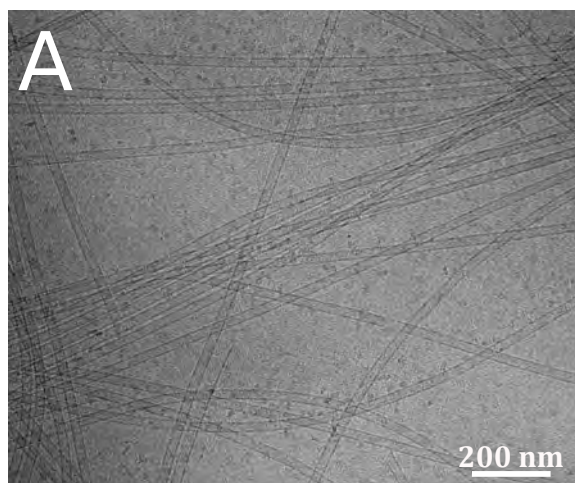


Figure S3: Cryo-TEM images (A & B) of Taxol stabilized MT solution. A solution of 0.2mM tubulin was polymerized for 35 min at 36°C in the presence of 4mM GTP. 0.2mM Taxol was then added and mixed using a truncated tip. The sample was incubated for additional 5 min. An aliquot was extracted, kept at 36°C for 70 min, until being vitrified and imaged.

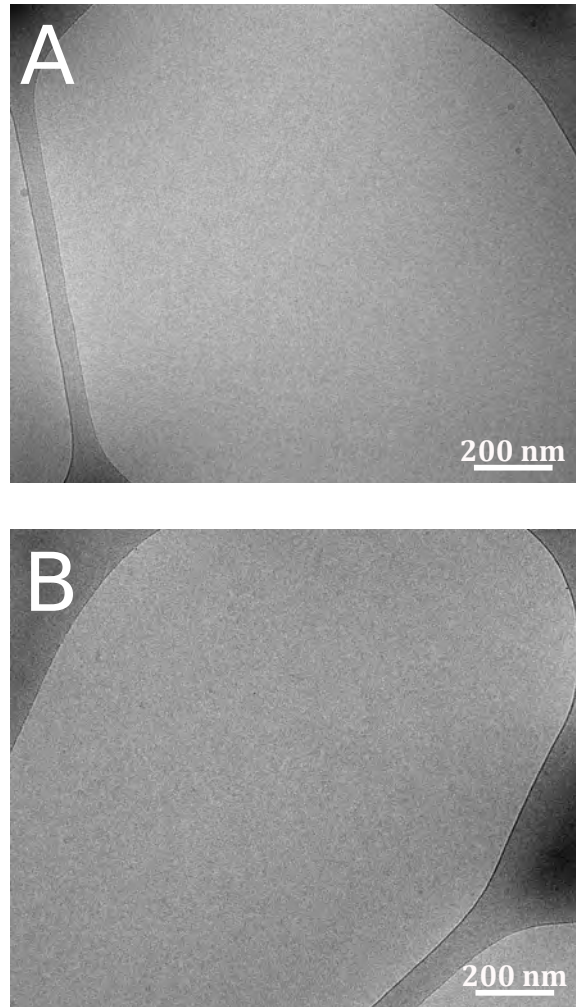


Figure S4: Cryo-TEM images (A & B) of Taxol stabilized MT solution supernatant. A solution of 0.2mM tubulin was polymerized for 35 min at 36°C in the presence of 4mM GTP. 0.2mM Taxol were then added and mixed using a truncated tip. The sample was incubated for additional 5 min. The Taxol stabilized MT solution solution was then centrifuged at 20800 g and 36°C for 30 min. Supernatant sample was extracted and kept at 36°C for 50 min, until being vitrified and imaged.

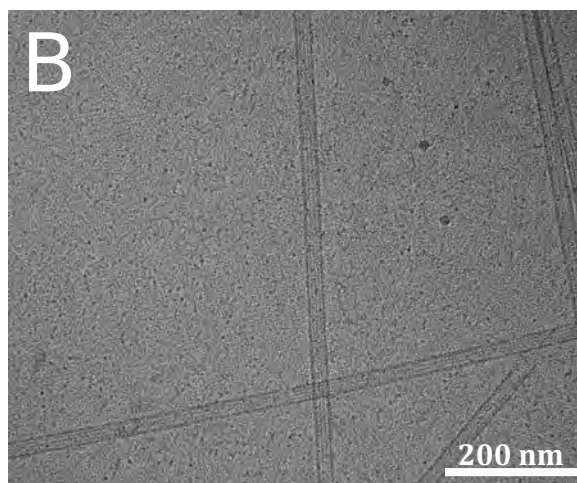
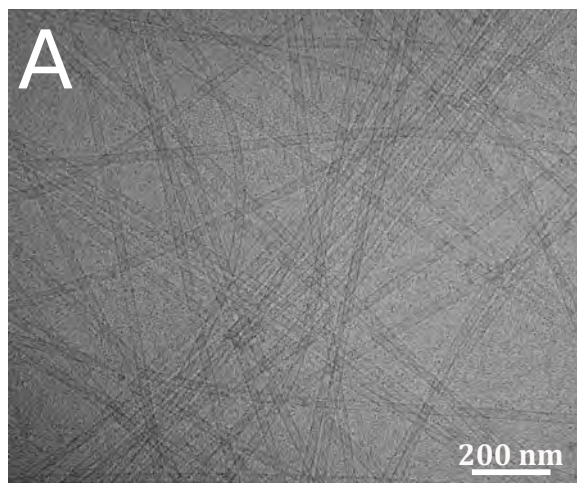


Figure S5: Cryo-TEM images (A & B) of GMPPCP stabilized MT solution. A solution of 0.2mM tubulin was polymerized for 35 min at 36°C in the presence of 4mM GMPPCP. An aliquot was extracted, kept at 36°C for 80 min, until being vitrified and imaged.

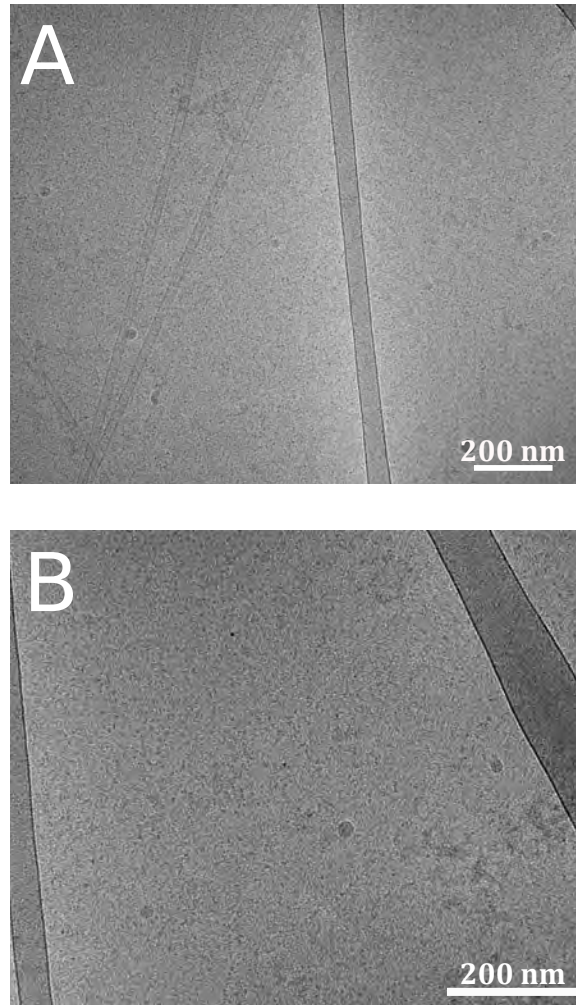


Figure S6: Cryo-TEM images (A & B) of GMPPCP stabilized MT supernatant. A solution of 0.2mM tubulin was polymerized for 35 min at 36 °C in the presence of 4mM GMPPCP. The GMP-PCP stabilized MT solution was then centrifuged at 20800 g and 36 °C for 30 min. Supernatant sample was extracted, and kept at 36 °C for 60 min, until being vitrified and imaged.

Finding the rotation angles of an object

To save computations, we bin copies of an object together when their orientation is identical. To find the final rotation angles of an object that has been rotated several times, relative to its initial lab axes directions: $(1, 0, 0)$, $(0, 1, 0)$, and $(0, 0, 1)$, we apply the same rotation on the lab axes unit vector. In other words, we multiply the rotation matrices and obtain the final rotation matrix:

$$\mathbf{XYZ} = \begin{bmatrix} x_1 & y_1 & z_1 \\ x_2 & y_2 & z_2 \\ x_3 & y_3 & z_3 \end{bmatrix} \quad (1)$$

To find the α, β , and γ rotation angles, in the range between $-\pi$ and π , we compare the \mathbf{XYZ} matrix with the rotation matrix:

$$\mathbf{A}(\alpha, \beta, \gamma) = \begin{bmatrix} \cos \beta \cos \gamma & -\cos \beta \sin \gamma & \sin \beta \\ \cos \alpha \sin \gamma + \cos \gamma \sin \alpha \sin \beta & \cos \alpha \cos \gamma - \sin \alpha \sin \beta \sin \gamma & -\cos \beta \sin \alpha \\ \sin \alpha \sin \gamma - \cos \alpha \cos \gamma \sin \beta & \cos \gamma \sin \alpha + \cos \alpha \sin \beta \sin \gamma & \cos \alpha \cos \beta \end{bmatrix}$$

and find the three angles.

To calculate the angles we use the function $\arctan(y, x)$ (the function `ATAN2` in C++), which gets the values of the \cos (for y) and the \sin (for x) of the relevant angle and returns the angle (in radians) in its correct quadrant, based on the sign of the two arguments. If both the \cos and the \sin are positive the angle is between 0 and $\pi/2$. If the \sin is positive and the \cos is negative the angle is between $\pi/2$ and π . If both are negative the angle is between $-\pi$ and $-\pi/2$, and if the \sin is negative and the \cos is positive then the angle is between $-\pi/2$ and 0 .

We then proceed as follows

$$\alpha_0 = \arctan(z_2, z_3)$$

We define $c_2 \equiv \sqrt{x_1^2 + y_1^2}$.

If $\alpha_0 > 0$:

$$\alpha_0 = \alpha_0 - \pi$$

$$\beta_0 = \arctan(-z_1, -c_2)$$

else

$$\beta_0 = \arctan(-z_1, c_2)$$

We define:

$$s_1 \equiv \sin(\alpha_0)$$

$$c_1 \equiv \cos(\alpha_0)$$

and then:

$$\gamma_0 = \arctan(s_1 \cdot x_3 - c_1 \cdot x_2, c_1 \cdot y_2 - s_1 \cdot y_3)$$

Finally we get that:

$$\alpha = -\alpha_0, \beta = -\beta_0, \gamma = -\gamma_0.$$

Scattering curves of supernatants

The dynamic and stabilized MT scattering curve of the buffers were subtracted from the scattering curves of the corresponding supernatant curves (see Figure 4). Figure S7 shows the buffer-subtracted scattering curves of supernatants of dynamic MT, taxol-stabilized MT, and GMPPCP-stabilized MT. The scattering curve from a solution of cold (unpolymerized) tubulin is shown for comparison.

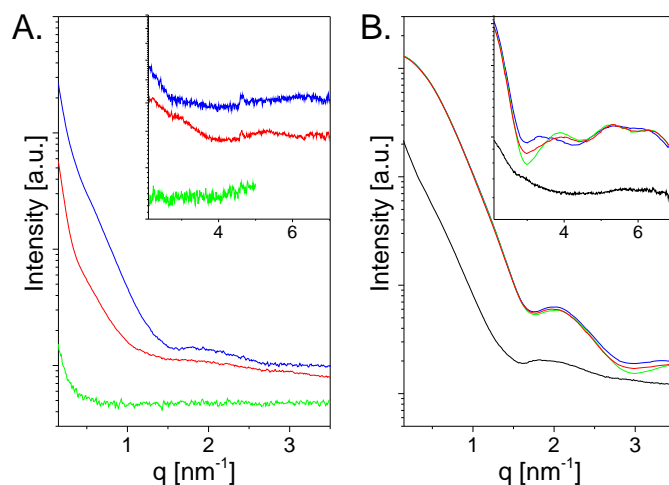


Figure S7: **A.** Buffer-subtracted scattering curves of the supernatants of dynamic (GTP) MT (red), taxol-stabilized MT (green), and GMPPCP-stabilized MT (blue). The measured supernatant and buffer scattering curves before subtractions are shown in Figure 4. **B.** The buffer subtracted scattering from a solution of 0.2 mM tubulin with 4 mM GTP at 5 °C (black curve) and atomic resolution models of GTP-, Taxol- and GMPPCP-tubulin, in red, green and blue, respectively. The atomic model were computed based on PDB IDs 3J6F, 3J6G, and 3J6E, respectively

Turbidity kinetic measurements

Tubulin incubation times before measurements were optimized for GTP polymerization at high protein concentrations. Applying the same assembly protocol to samples for which GTP was replaced by GMPPCP resulted in a significantly slower kinetics, as demonstrated in Figure S8. This may have affected the structures comprising the supernatant. After the samples were centrifuged and supernatant was separated from the MT pellet, the supernatant was incubated at 36 °C for few tens of minutes before measurements were performed. During this time, free nucleotide and tubulin dimer molecules above the MT assembly critical concentration were present and MT filaments could assemble, as demonstrated in Figures 3B and S6. Figure S8 also demonstrates the effect of tubulin concentration on the assembly kinetics and steady state, implying that a longer incubation period should be used for lower tubulin concentrations.

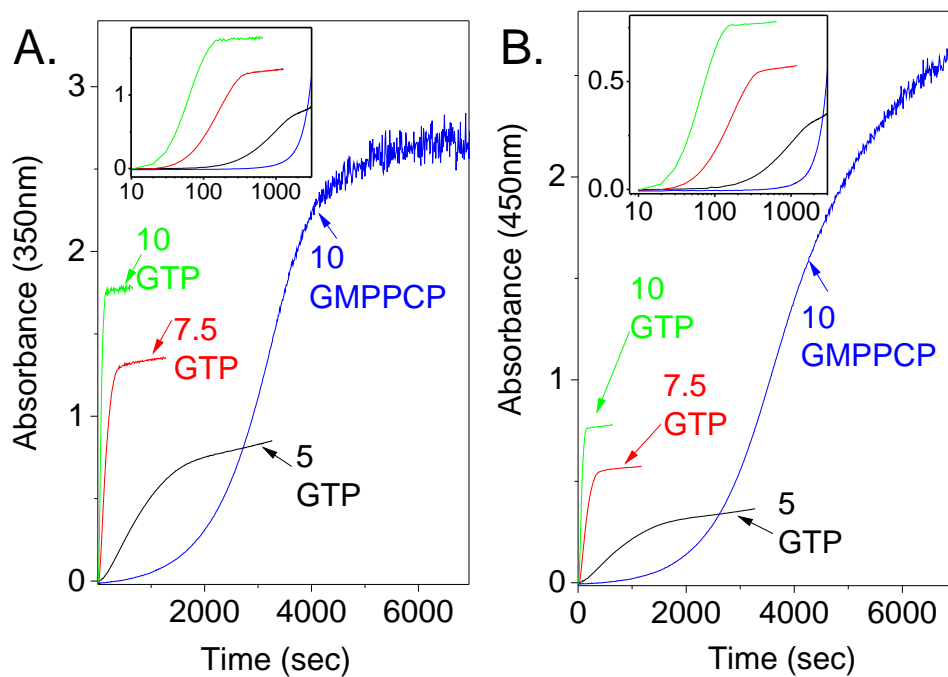


Figure S8: Turbidity kinetic measurement of tubulin assembly at 36 °C for different tubulin concentrations (in units of mg/mL) in the presence of 4mM nucleotide, as indicated in the figure. Absorbance was measured simultaneously both at 350 nm (A.) and 450 nm (B.). The insets show the incubation phase on an expanded Log scale.

Instrument resolution effect

The effect of instrument resolution is examined in Figure S9.

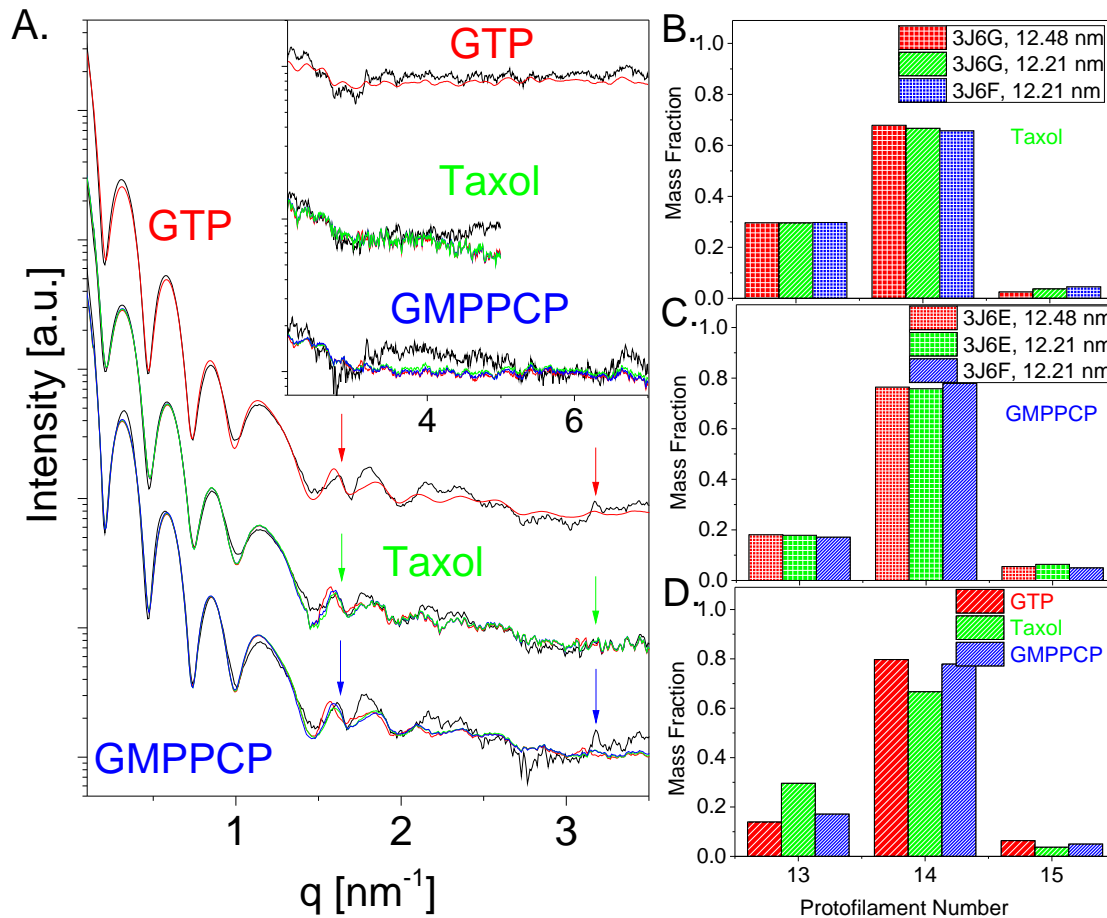


Figure S9: Fitting the data of Figure 5, to the same models of Figure 5, however, the standard deviation, σ_q , of the Gaussian instrument resolution function was set to the upper limit of 0.02 nm^{-1} .

Additional solution X-ray scattering data

Measurements similar to those in Figure 5 were repeated at ESRF and Lund Synchrotrons and were analyzed as in Figures 5, 7, or 8. The results are shown in Figure S10.

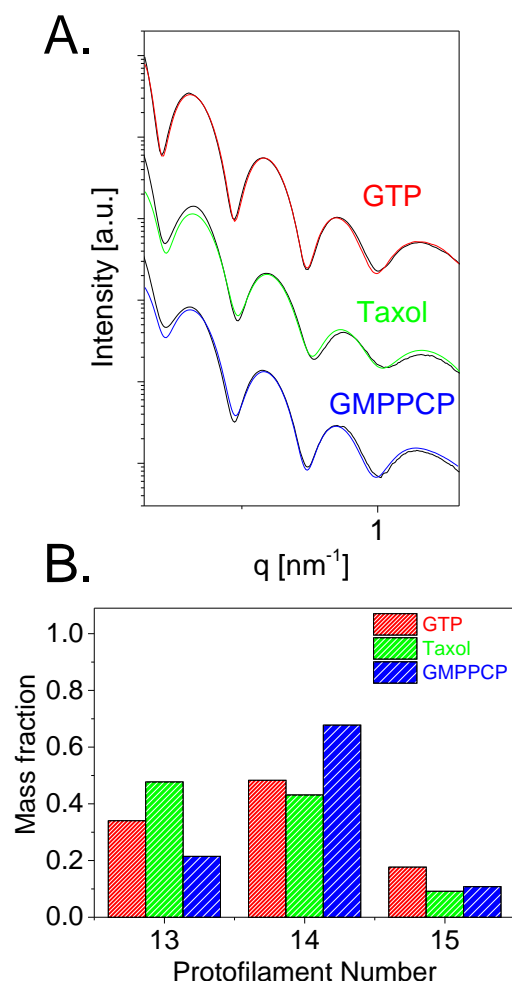


Figure S10: Supernatant-subtracted solution X-ray scattering data and atomic models of dynamic and stabilized MT. **A.** Supernatant subtracted scattering intensity black curve of dynamic (GTP) MT (top) was measured at ID02 beamline in ESRF (Grenoble). Taxol-stabilized MT (middle) and GMPPCP-stabilized MT (bottom) were measured in I911-SAXS beamline in MaxII Synchrotron (Lund). The red, blue, and green curves are the computed scattering curves based on a linear combination (Eq. 7) of different atomic MT models and the curves of Figure S7. All the models were convolved (Eq. 6) with an estimated Gaussian instrument resolution function with standard deviation, σ_q , of 0.01 nm^{-1} (dynamic MT fitting) and 0.025 nm^{-1} (stabilized MT fitting). In each model, the dimers were arranged in a 3-start left-handed helical lattices with radii to the geometric center of the dimer atomic coordinates, R , of 11.05, 11.9, and 12.75 nm, corresponding to 13, 14, and 15 protofilaments. 12 protofilaments ($R = 10.2 \text{ nm}$) and tubulin dimer models were included in the models but their mass fraction was negligible. Each protofilament contained 16 tubulin dimers. The mass fractions were determined by fitting a linear combination of five models (MT with 12, 13, 14, and 15 protofilaments and tubulin dimer) and the relevant supernatant solution and cold tubulin dimer signals (Figure 7S) to the scattering data. **B.** The mass fraction distributions of the contributing models that best fitted the data. The colors of the computed curves in **A.** match the colors in the mass fraction bar-diagram.

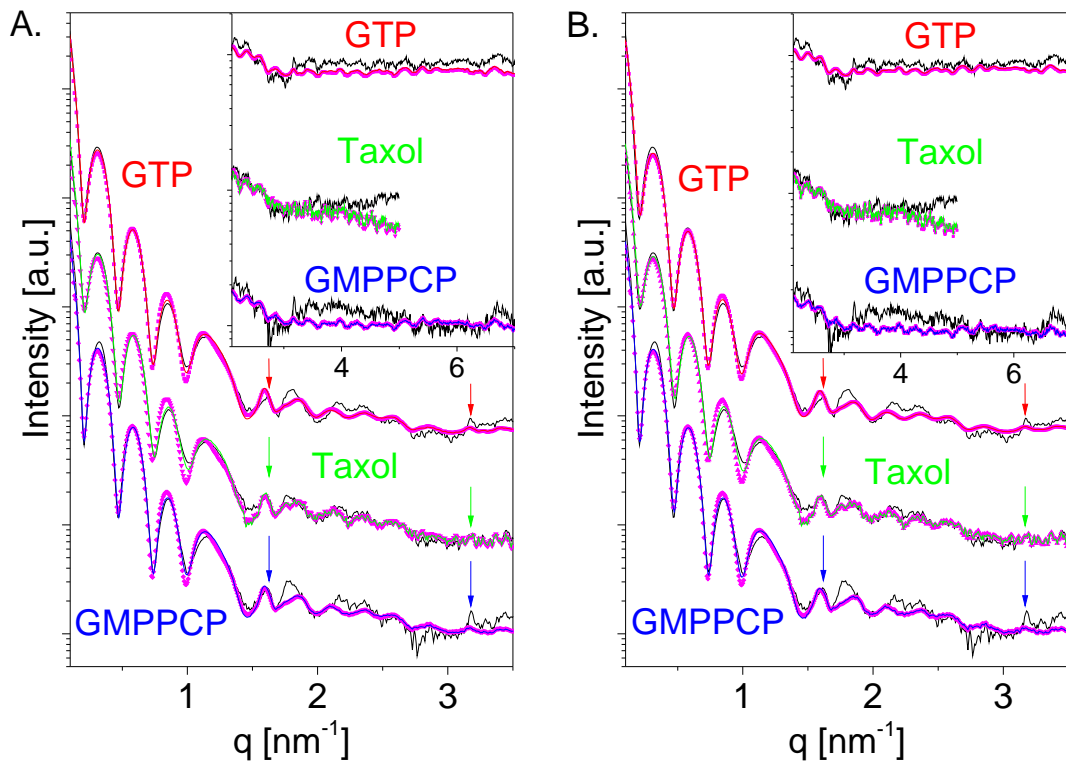


Figure S11: Comparing single- with multiple-population atomic models of dynamic- and stabilized-MT. The analysis is similar to Figure 7, however, the pink curves assume that all the population contained only MT with 14 protofilaments, after the contribution of background-subtracted supernatant, cold-tubulin solution and the dimer models (Figure S7) were taken into account. In **A** σ_q was 0.01 nm^{-1} and in **B** σ_q was 0.02 nm^{-1} .